Chapter 12
Effect of Different Test Setup Configurations on the Identification of Modal Parameters from Digital Image Correlation

L. Marchetti, D. Mastrodicasa, E. Di Lorenzo, S. Manzato, L. Bregant, B. Peeters, and P. Lava

Abstract Over the past few years, the application fields for digital image correlation (DIC) have significantly broadened and are now extensively used not only for material characterization and deformation analysis but also for vibration and dynamic testing. The key advantage over more traditional technologies such as accelerometer- or laser-based measurement is the fact that all points of interest can be measured at once or over a limited number of repetitions without mass loading the structure or having to deal with complex cabling scenarios. While qualitative analysis, such as operational deflection shapes, proved to be very successful and straightforward, performing classical modal analysis on frequency response functions between a load cell signal and the deformations obtained by applying digital image correlation still requires extra care when setting up the experiments. In this paper, the effect of different cameras, camera settings, excitation levels, and speckle pattern on the modal parameters of a simple plate structure will be investigated and compared with classical acceleration measurement. The results will also be compared with numerical simulations where the accuracy of the mode shapes can be easily and quantitatively assessed.

Keywords Digital image correlation · FRF testing · Speckle patter · Modal analysis

12.1 Introduction

Nowadays, testing and validation for mechanical numerical models are mostly performed using a discrete number of transducers (e.g., accelerometers, strain gauges, fiber optics, etc.), which can only provide measurements at finite locations. Moreover, on lightweight structures, the accelerometers might impact the measurement because of mass loading. For these reasons there have been a growing research and industrial interest in contactless measurement technologies. Laser Doppler vibrometry is a quite established solution [1], but recently techniques based on images are attracting more and more interest and digital image correlation (DIC) in particular has recently received special attention in the structural dynamics field as a full-field measurement technique [2, 3]. In particular, DIC for vibration analysis is mostly performed on aerospace and automotive components [4–8] and rotating structures [9] like turbine blades [10] and helicopter rotors [2].

If the structure's high frequency behavior is investigated, high-speed cameras are needed in order to respect the Nyquist-Shannon's theorem. The principal drawback is that high-speed cameras present lower image resolution, which limits the

L. Marchetti
Siemens Digital Industries Software, Leuven, Belgium

Department of Mechanical Engineering, Università degli Studi di Trieste, Trieste, Italy

D. Mastrodicasa
Siemens Digital Industries Software, Leuven, Belgium

Acoustic & Vibration, Vrije Universiteit Brussels, Brussels, Belgium

E. Di Lorenzo · S. Manzato (✉) · B. Peeters
Siemens Digital Industries Software, Leuven, Belgium
e-mail: simone.manzato@siemens.com

L. Bregant
Department of Mechanical Engineering, Università degli Studi di Trieste, Trieste, Italy

P. Lava
MatchID, Ghent, Belgium

D. Di Maio, J. Baqersad (eds.), *Rotating Machinery, Optical Methods & Scanning LDV Methods, Volume 6*, Conference Proceedings of the Society for Experimental Mechanics Series, https://doi.org/10.1007/978-3-030-76335-0_12

vibration amplitude that can be measured. Higher resolution is usually available on lower-speed camera, so depending on the application, a compromise between speed and quality must be sought. The solution that allows to analyze high-frequency vibrations with high-quality images is the under-sampling technique [11, 12]. With this method it is possible to overcome the low sampling rate of high-resolution cameras by under-sampling and remapping the time histories to measure above their Nyquist frequency.

To measure FRFs, the camera images need to be perfectly synchronized with the excitation force and time-stamped using the same clock. This can be achieved by using external triggers on the camera, using external absolute clocks or by using reference signals that can be later on used to align the images with the samples acquired by the main data acquisition system. With the cameras used in this paper, using alignment with an artificial signal was the only option available.

In this paper DIC technique is used to get the full-field displacement time histories of three metal plates. These data are then processed and analyzed in order to obtain the FRFs and modal parameter [13] and will be validated against results from standard accelerometer measurements. The effect of different test setup configurations on the FRFs and modes will be investigated. In particular, the influence on results of the type of excitation used, the number of averages used for the calculation of FRFs, the frequency resolution, and the kind of speckling used on the plates will be evaluated.

12.2 Aliased Acquisition with Low-Speed Camera

In this study, the measurements were performed using two FLIR Blackfly S USB3 5 MP cameras, running at a max of 75 fps at max resolution. The measurements were also performed by directly streaming the images to the PC; this has the advantage that the images are already available, but if no dedicated is available, the camera speed is limited to max 25 fps because of the limited data transfer capacity of regular USB3 ports. Since the structure has been excited using periodic chirp and pseudo random signals having a maximum frequency higher than the camera frequency, the reconstruction technique is used.

This method is based on the requirement that the signal analyzed for the reconstruction must be periodic; under this assumption, it is possible to reconstruct it at a lower frequency using signal aliasing. The process is illustrated in Fig. 12.1. To measure the signal in blue in the left plot, at a frequency $f = f_{\text{signal}}$, a signal at sampling frequency $f_{\text{sample}} < f_{\text{signal}}$ can be used (purple signal in the center). This signal's frequency f_{r} is related both to f_{signal} and f_{sample}, and it is equal to:

$$f_r = f_{signal} \cdot f_{sample} \cdot \left(f_{sample}^{-1} - f_{signal}^{-1} \right) \tag{12.1}$$

The reconstructed signal has the same shape of the original signal, but it is scaled along the time axis. The purple signal is described by the equation:

$$S_r(t) = S_{signal} \cdot \left(\frac{f_r}{f_{signal}} \cdot t \right) \tag{12.2}$$

Using Eq. (12.2) it is now possible to obtain Eq. (12.3) and to reconstruct one period of the desired signal, as shown in Fig. 12.1 (right).

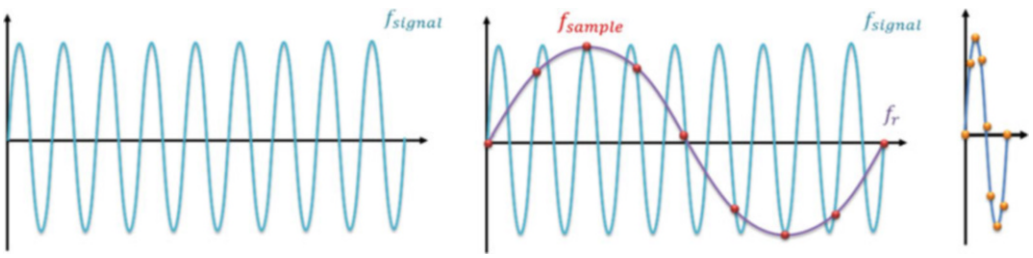

Fig. 12.1 Signal reconstruction process: (left) original signal; (center) original and sampled signal; (right) reconstructed signal

$$S_{artif}(t) = S_r \cdot \left(\frac{f_{signal}}{f_r} \cdot t \right) \tag{12.3}$$

Using this principle, it is possible to sample a very high-frequency signal with cameras operating at a low sample rate and then reconstruct it after the measurement. The main drawback of this approach is that the duration of the test is much longer than when using high-speed cameras, as the signal must be repeated until all samples to reconstruct the original signal have been acquired.

12.3 Experimental Setup

12.3.1 Test Item

The objective of this study is to perform a full-field modal analysis on a metal plate estimating FRFs using DIC. Since the effects of the test setup configurations are important to compare the influence of the different speckles, three different plates have been used. The original idea was to have three identical plates and to compare the results obtained on different plates using different settings. A big plate was then cut to obtain three plates with the same dimension (327 mm × 273 mm × 0.8 mm). However, as it will be shown later, the plates were hand-cut, resulting in local plastic deformations that influenced the structural properties of each one. Consequently, the analysis will be run on each of the three plates independently, and no-cross comparison, as was originally foreseen, can be performed.

Different speckle patterns were applied on the surface of each plate, as shown in Fig. 12.2, in particular:

- Plate 1: paint was sprayed on the plate and then dots were drawn with a pen.
- Plate 2: dots were printed on A4 paper. Then the plate was speckled using these A4 paper sheets glued on it.
- Plate 3: paint was sprayed on the plate and then dots were drawn with a pen on half plate. On the other half, speckle printed on paper has been glued.

12.3.2 FRF Testing

For each plate, reference properties were estimated by measuring FRFs using a shaker excitation at the center point of the plate before the speckle pattern was applied. The sensor setup is shown in Fig. 12.2, where the two accelerometers corresponding to the orange dots and the impedance head by the blue one are displayed on the three plates. The driving point FRFs measured on the three plates are shown in Fig. 12.3. As already mentioned, the three plates show a significantly different behavior in the complete frequency range. Due to the low weight and small thickness, even small differences cause significant effects on the natural frequencies, making it impossible to quantitatively compare the results between the three plates.

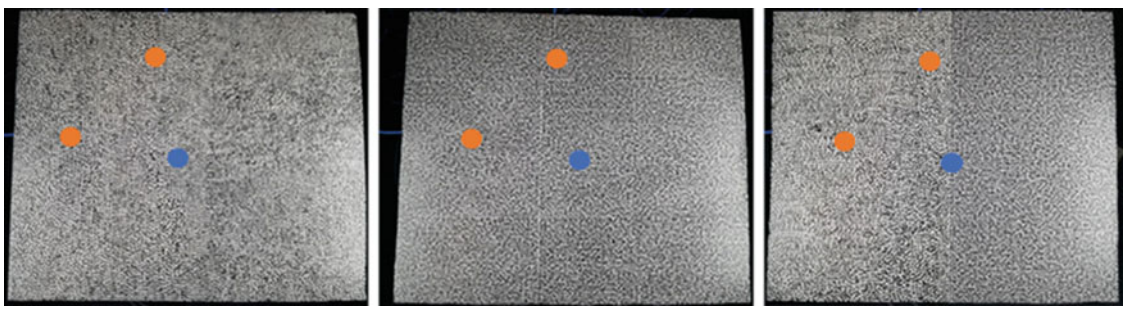

Fig. 12.2 Speckled plate. (Left) Plate 1 with painted speckle. (Center) Plate 2 with printed speckle. (Right) Plate 3 with half painted and half printed speckle. The blue dot indicates the excitation location (with impedance head), while the orange dot indicates response measurement locations with accelerometers

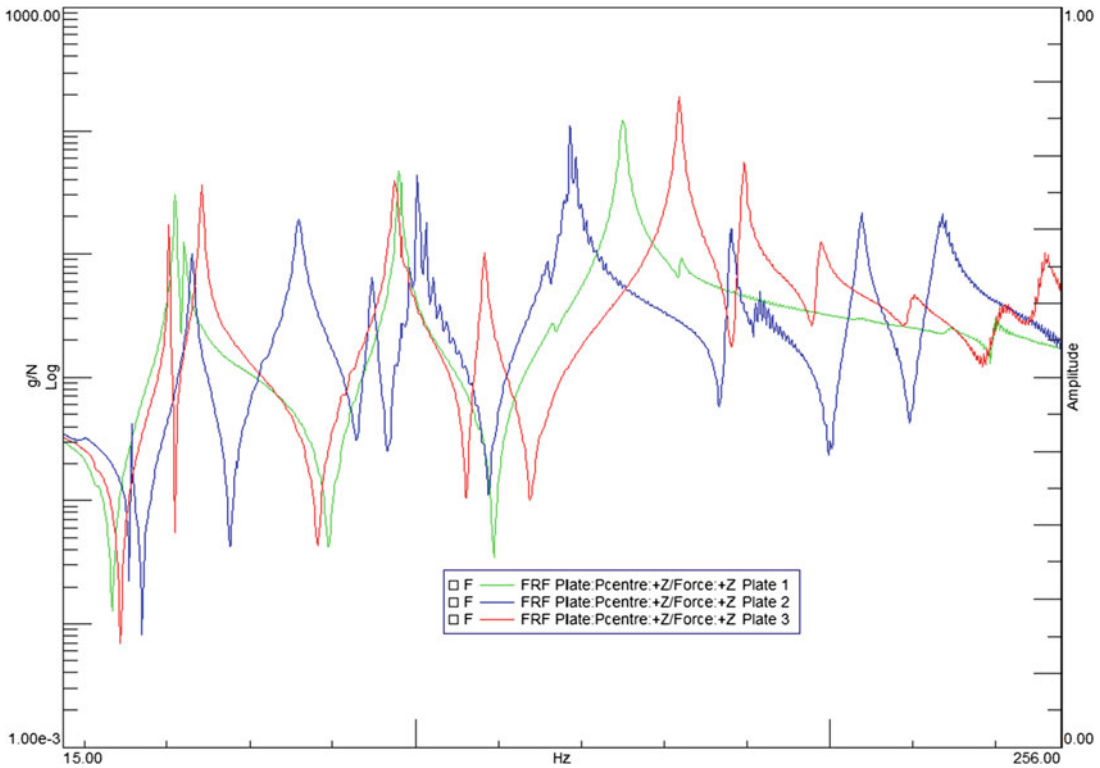

Fig. 12.3 Driving point FRFs measured on the three plates

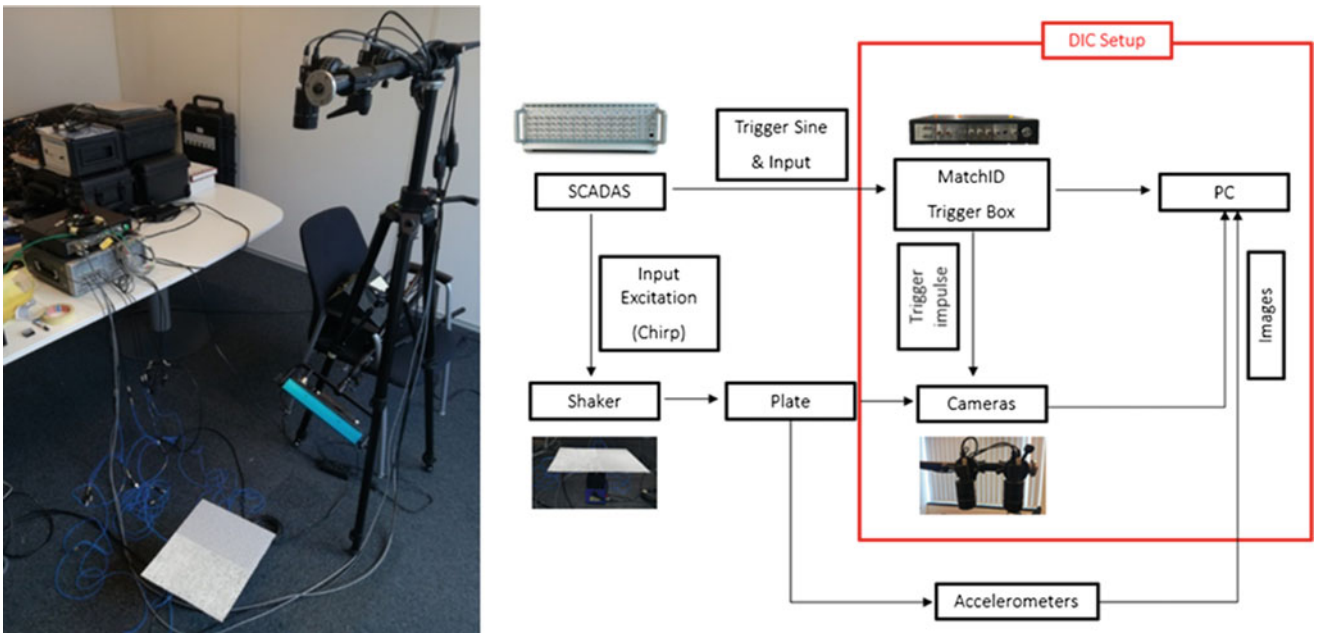

Fig. 12.4 Experimental setup with a schematic description of the connection between the different elements

12.3.3 Camera Setup/Measurement Chain

The experimental setup is shown in Fig. 12.4. The plate was excited using a shaker positioned at the center of the plate, while the response was captured using a pair of DIC cameras in a stereo configuration and three accelerometers placed under the plate.

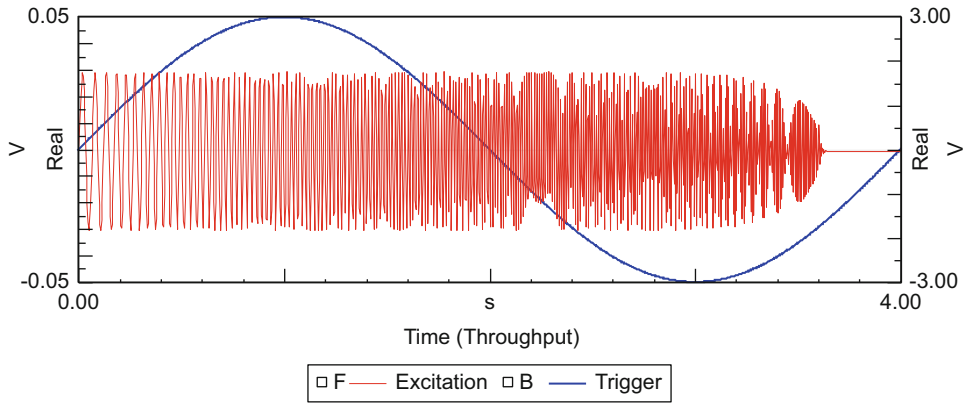

Fig. 12.5 Example of an excitation (chirp) and trigger signals

Table 12.1 Overview of excitation profiles

Technique	Pro	Cons
Chirp	Easy, quick test	Results not good
Pseudo random	1 realization, repeatable	More deterministic
Pseudo random averages	Repeatable, averages	More deterministic

The cameras were triggered by the MatchID TriggerBox, while the shaker was driven by the DAC of a Simcenter SCADAS that was also used to record the force and acceleration signals from the sensors. A reference signal was exchange between the two systems to synchronize the acquisition.

The DAC module of Simcenter SCADAS is used to generate two signals. One is used to excite the structure and must be a stationary and periodic signal. In this study, both chirp and pseudo random signals were used Table 12.1. The second generated signal is a sync signal, which is sent to the Triggerbox and used as a trigger. This is typically a sine whose period spans an integer number of excitation blocks. An example of these signals is shown in Fig. 12.5. The sine signals can then also be used to align the samples acquired in the two systems before applying post processing.

12.4 Results

In this section, the different experiments and the corresponding results will be presented. As the main objective is to assess the quality of the FRFs measured with DIC, the results will be compared with the FRFs obtained with the accelerometers in Fig. 12.2. In both cases, the FRFs are computed using the force signal measured with the load cell at the interface between the shaker and the plate.

The first goal is to find the excitation profile that gives the best results in terms of system's response, by comparing the DIC FRFs to those calculated using accelerometers. The second is to tune the level and bandwidth of the excitation to have displacements which are big enough for the cameras, but without overexciting the system.

12.4.1 Type of Excitation

The experiments started on plate 2 (the plate with the printed speckle pattern). The first excitation was a chirp of 4 s in the bandwidth of 15–128 Hz. At the same time, a sine with the same period of 4 s was sent to the TriggerBox to provide the timing for the aliased acquisition and the following reconstruction. The FRFs obtained with DIC identify the peaks correctly, but the magnitude and in particular the phase are noisy, due to the fact that no averaging is performed. Figure 12.6 shows the FRF calculated at the center point of plate 2 in red.

In order to improve the results, a pseudo random signal of 5.12 s and bandwidth 15–100 Hz was used. Also in this case, 1024 images were acquired to reconstruct the signal. The resulting FRF at the center point is now displayed in blue in

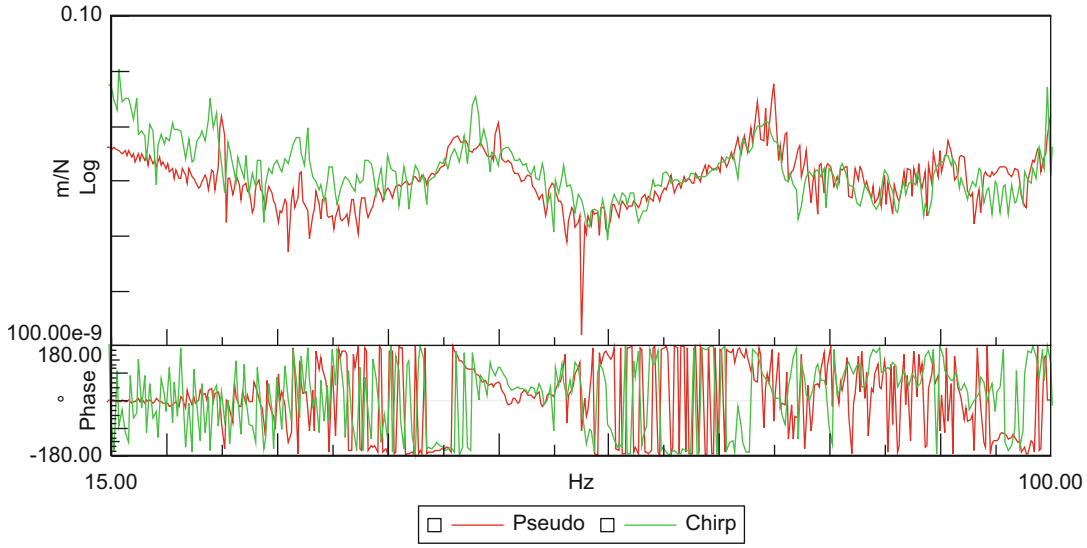

Fig. 12.6 FRF measured at the center of plate 2 with DIC for different excitations: Chirp (red) and pseudo random (blue)

Fig. 12.6. While the FRF remains noisy, the peaks are correctly captured, and, most importantly, the phase is more stable at lower frequencies. Because of the enhanced properties of a pseudo random signal (controlled amplitude and phase in the generation of the signal and inherently periodic excitation) versus a chirp, this was chosen as the reference excitation profile for the remaining of the investigation.

12.4.2 Number of Averages

The FRFs shown in Fig. 12.6 clearly show that averaging is required to further minimize noise and ensure that modal analysis can correctly extract the modal parameters from the data. As one of the limitations of DIC is the computational effort required to process the images, the effect of averaging was performed by fixing the number of images to 1024 and using the available samples to describe more cycles. The following tests were performed:

- One average with a block of 5.12 s, bandwidth 15–100 Hz, and resolution of 0.195 Hz.
- Two averages with block of 2.56 s, bandwidth of 15–100 Hz, and resolution of 0.391 Hz.
- Four averages with block of 1.28 s, bandwidth of 15–100 Hz, and resolution of 0.781 Hz.

The results of the different test will now be assessed in terms of modal parameters. Hence, they will be compared with the results obtained by processing the accelerometers' FRFs. To ensure consistency, the accelerometers were always attached to structure during the whole experimental campaign.

Figure 12.7 shows the stabilization diagram obtained by processing the FRFs with, respectively, two and four cycles. The case with only one cycle was not displayed as the results were noisy, and to identify the modes of interest, a very high model order had to be specified. The picture shows how the stabilization diagram built from the four averages FRFs is much cleaner than the other, allowing to correctly identify the five modes expected in this frequency region. While the same modes could be identified also using only two averages, the model order had to be doubled, and many more spurious poles could be observed. Although not reported here, the FRFs obtained by averaging 4 times had a much cleaner phase relation in the frequency range of interest.

.

The frequency and damping of the identified modes in the three DIC scenarios are compared in Table 12.2 with those obtained by processing the accelerometer FRFs. The results obtained with the four averages FRFs are those that best match the one from the accelerometers, which are considered here the reference. It can be then concluded that, as expected, sacrificing frequency resolution for a higher number of averages can significantly improve the quality of the estimated modal parameters. While for the first four modes the damping is accurately estimated, for mode 5 it is significantly underestimated if compared to the one obtained from the accelerometers. This is expected as the FRFs at higher frequency are still noisy,

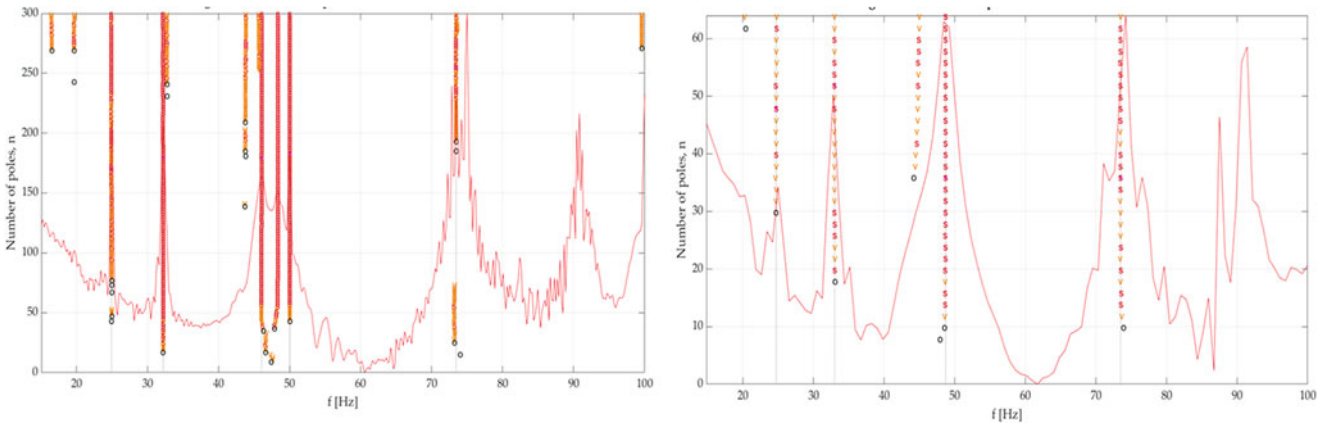

Fig. 12.7 Stabilization diagram built on the FRFs from the two cycles (left) and four cycles (right) test

Table 12.2 Comparison of modal parameters from accelerometer and DIC FRFs

Modes	Accelerometers		DIC 4 cycles		DIC 2 cycles		DIC 1 cycle	
\	f_n [Hz]	d%	f_n [Hz]	d%	f_n [Hz]	d%	f_n [Hz]	d%
1	24.2	1.02	25.1	1.02	25.7	0.10	20.8	1.17
2	31.7	0.15	32.0	0.11	32.6	0.13	33.3	0.08
3	47.1	1.89	47.1	1.41	48.0	1.36	46.1	1.29
4	73.8	0.52	73.8	0.52	74.2	0.15	77.5	0.05
5	89.5	0.49	91.4	0.07	92.1	0.03	92.2	0.05

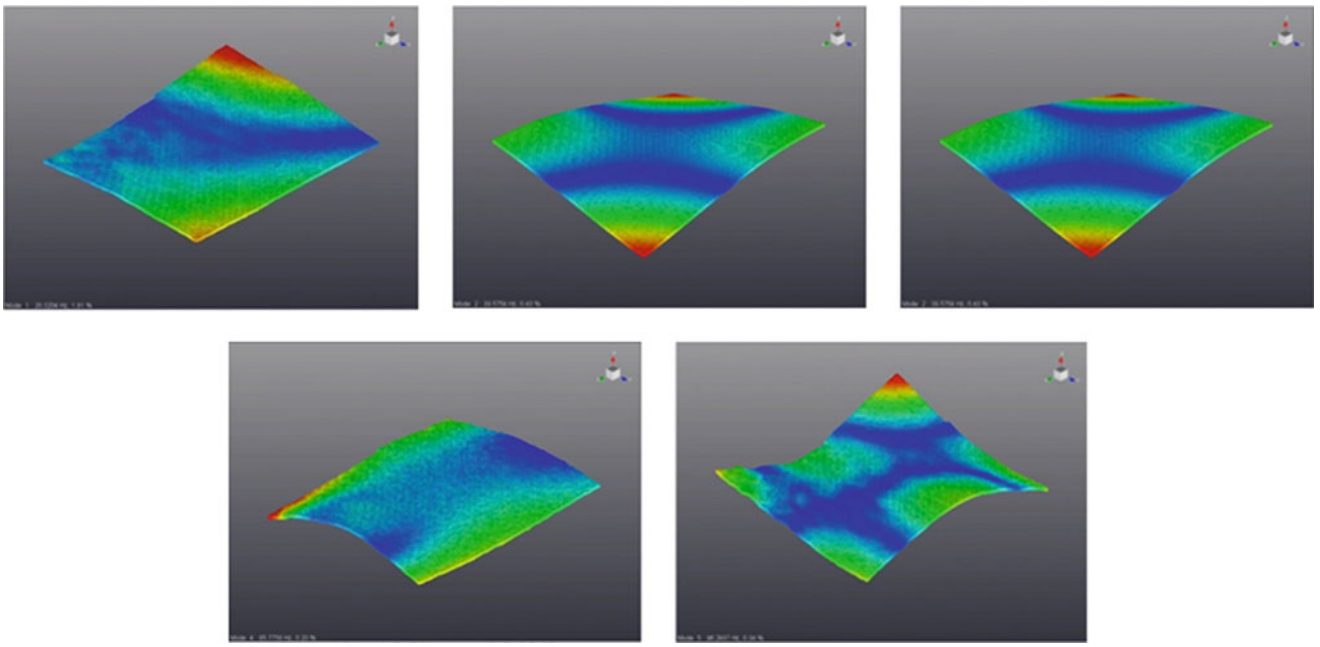

Fig. 12.8 Identified mode shapes for the five resonances identified in the frequency range of interest

affecting the stability of the estimation and causing the damping to be underestimated. The identified shapes for the four averages case are shown in Fig. 12.8.

A further validation of the obtained results can be obtained by comparing the DIC FRFs directly with the ones measured with the accelerometers. The DIC FRFs have been extracted trying to match the locations of the accelerometers and impedance head as shown in Fig. 12.2. As DIC usually extracts the displacements, after calculating the FRF, they have been differentiated twice to extract the corresponding accelerations. The results are shown in Fig. 12.9. The point which shows the best agreement between the two measurement techniques is point 2, which is the point at the center of the plate. The main

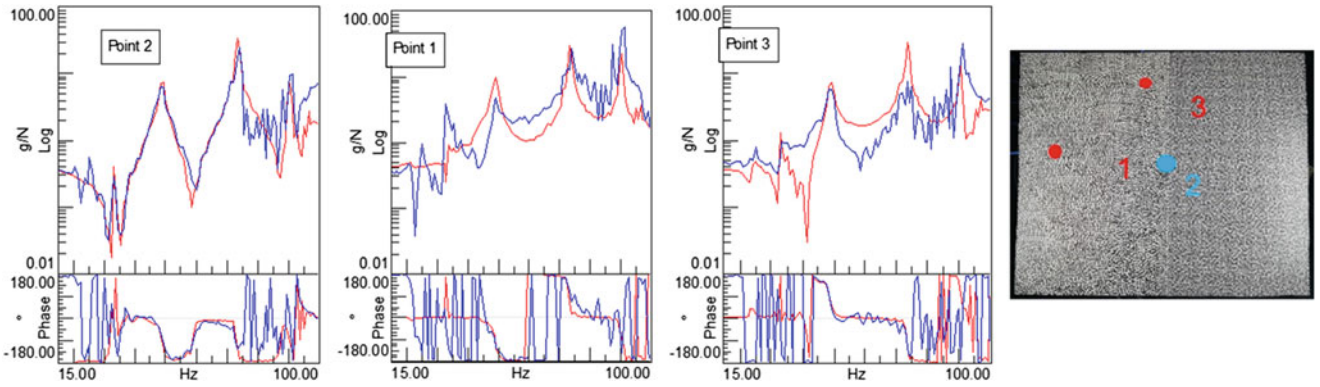

Fig. 12.9 Comparison between DIC (blue) and accelerometer (red) FRFs. Point locations on the plate are shown in the right

Table 12.3 Accelerometer vs DIC modes for plate 3 between 100 and 400 Hz

Modes	Accelerometers		DIC	
\	f_n [Hz]	d%	f_n [Hz]	d%
1	112.9	0.41	115.0	0.44
2	127.9	0.73	127.5	0.66
3	160.9	0.45	160.6	0.24
4	175.6	0.43	176.2	0.95
5	196.6	0.40	197.9	1.17
6	211.9	0.62	/	/
7	231.2	1.59	235.8	0.01
8	246.5	0.36	252.0	0.17
9	301.7	0.29	301.0	0.13
10	321.8	1.56	316.8	0.69
11	338.9	0.74	338.2	0.52
12	368.9	0.46	372.5	0.08

peaks match with those obtained from the accelerometers, both in frequency and in amplitude. In between resonances, the FRF is noisier, but this is limited impact in a modal analysis context. On the other points, while the peaks still align in terms of frequency, the amplitude shows some deviation and the response is generally noisier.

12.4.3 Extended Frequency Range

While testing plate 3 (half painted and half printed speckle), the excitation range was extended to 400 Hz to see whether the cameras could still capture displacement at these higher frequencies. To compensate for the quadratic decrease of displacements as the frequency increases, the excitation level had to be slightly increased compared to the previous test. Additionally, it was observed that if the excitation was applied in the whole range, from 15 to 400 Hz, the lower-frequency response was masking the dynamics above 100 Hz, with very noisy responses and response levels below the noise floor of the cameras. It was then decided to limit the excitation from 100 to 400 Hz, since the dynamics at lower frequencies have been already analyzed. This allowed to decrease the noise floor for the cameras, ensuring a better dynamic range in this frequency region. In total, 11 modes out of the 12 identified with the accelerometers were extracted, with damping values reasonably matching the reference ones. Table 12.3 gives a comparison of the frequency and damping extracted with the two methods, while Fig. 12.10 shows some of the shapes identified. In particular, the modes shapes extracted at all points (approx. 9000) allows to visualize the deformation shape very accurately, with a spatial resolution that would be nearly impossible to achieve with accelerometers.

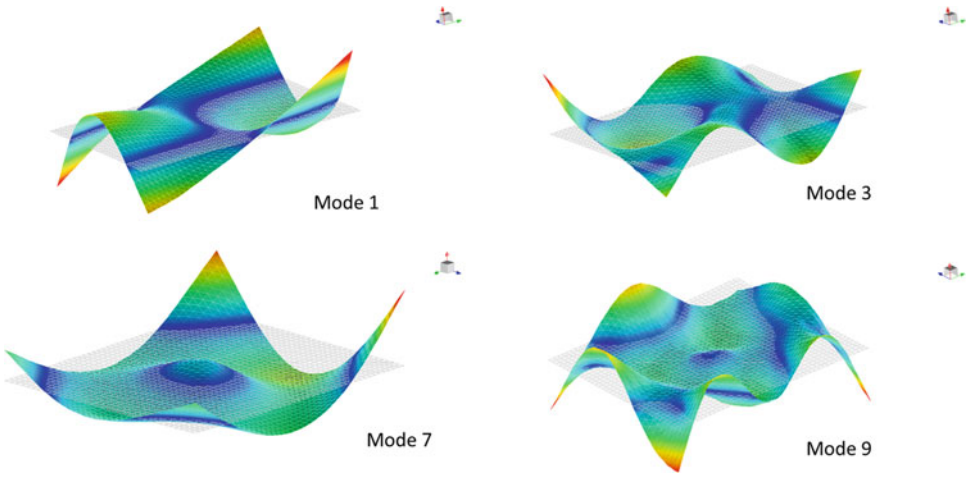

Fig. 12.10 Deformation shapes for some of the modes in Table 12.3

Table 12.4 Effect of speckle pattern on modal parameters of plate 3

Modes	Frequency			Damping		
\	No speckle	Paint	Paint + paper	No speckle	Paint	Paint + paper
\	[Hz]	[Hz]	[Hz]	%	%	%
1	40.5	39.2	39.1	0.1	0.04	2.91)
2	48.5	47.7	47.2	0.61	0.81	1.39
3	94.9	93.1	92.7	0.32	0.22	0.31
4	116.6	112.9	112.8	0.42	0.41	0.35
5	130.6	127.9	127.0	0.61	0.73	0.60
6	163.7	160.9	160.8	0.29	0.45	0.52
7	179.1	175.6	174.6	0.20	0.43	0.47
8	197.6	196.6	196.1	0.43	0.40	0.56
9	219.4	211.9	212.3	0.63	0.62	0.65

12.4.4 Effect of Speckling the Surface

Speckling the surface of a specimen could affect the structure's response, in particular if the object is light and thin like these plates. In order to evaluate the impact of the speckle, natural frequencies and damping have been identified on each plate before and after applying the speckle pattern. The analysis was carried out, in this case, using the FRF measured from the accelerometers. The locations of the accelerometers and the layout of the cables were carefully controlled between the different experiments, to limit as much as possible the impact of these factors on the results.

The results obtained on plate 3 are shown in Table 12.4. The table shows the results of modal analysis on FRF acquired before any speckles was applied, after applying the layer of paint and finally after gluing the printed speckles on half of the plate. By looking at the frequencies, it can be observed that adding more and more layers consistently decreases the estimated natural frequency, as expected when increasing the mass of the structures. In this case, where the plate was very light, this can cause natural frequency to shift 3–4 Hz for modes 4 and 5. Such variations are in line with the effect of adding locally few grams of mass on an FE model with equivalent properties.

For damping, in general it can also be observed that damping increases as the added material increases. Also in this case, however, the impact of adding accelerometers and cables on lightweight and lowly damped structure would cause similar variations. Similar trends were observed on the other two plates as well, so the results are omitted.

12.5 Conclusion

In this paper, the use of DIC for modal analysis is investigated. Different experiments were performed on a set of lightweight aluminum plate mounted on a shaker to analyze the effect of different setup and measurement options on the results.

First of all, it was observed that the type of excitation and the number of averages have a significant impact on the quality of the measurement and the FRFs. When using the aliased acquisition with low-speed cameras, it is of paramount importance that the excitation and response are as consistent as possible throughout the test. Using deterministic and controlled excitation such as pseudo random (multisine) profiles can significantly improve the quality of the data. Another important element is the number of averages to reduce noise. Finding the right balance between number of averages and computational time required for the DIC processing is important, but in general it was concluded that some compromise can be taken on the frequency resolution to obtain higher-quality data and more accurate modal estimates. When designing the experiment, the frequency range of interest was also shown to have an impact on the results. In general, it is suggested to repeat the test in different bandwidths, possibly progressively increasing the level to compensate for the lower displacement level at higher frequencies and avoid that low-frequency responses dominate the behavior at higher frequency.

Finally, applying speckle pattern on such a low weight structure was shown to have a limited impact on the results. Natural frequencies decreased due to increased mass and damping increased because of the extra layers of material applied, but these variations are in line with those caused by local accelerometers and cables.

References

1. Phillip, L., Reu, L., Rohe, D. and Jacobs, L.: Stereo-DIC vs 3D scanning LDV for modal. *Sandia National Laboratories*
2. Di Lorenzo, E., Lava, P., Balcaen, R., Manzato, S., Peeters, B.: Full-field modal analysis using high-speed 3d digital image correlation. J. Phys. **1149**(12), 012007 (2018)
3. Srivastava, V., Patil, K., Baqersad, J., Zhang, J.: A multi-view DIC approach to extract operating mode shapes of structures. Structural Health Monitoring, Photogrammetry & DIC. **6** (2019)
4. Molina-Viedma, A., Lopez-Alba, E., Felipe-Sese, L., Diaz, F., Rodriguez-Ahlquist, J.: Modal parameters evaluation in a full-scale aircraft demonstrator under different environmental conditions using hs 3d-dic. Materials. **11**, 230 (2018)
5. Seguel, F., Meruane, V.: Damage assessment in a sandwich panel based on full-field vibration measurements. J. Sound Vib. **417**, 1–18 (2018)
6. Bharadwaj, K., Sheidaei, A., Afshar, A., Baqer, J.: Full-field strain prediction using mode shapes measured with digital image correlation. Measurement. **139**, 326–333 (2019)
7. Galeazzi, S., Chiariotti, P., Martarelli, M., Tomasini, E.: 3d digital image correlation for vibration measurement on rolling tire: procedure development and comparison with laser Doppler vibrometer. J. Phys. Conf. Ser. **1149**, 012010 (2018)
8. Ha, N.S., Vang, H.M., Goo, N.S.: Modal analysis using digital image correlation technique: an application to artificial wing mimicking beetle's hind wing. Exp. Mech. **55**, 989–998 (2015)
9. Yashar, A., Ferguson, N., Tehrani, M.G.: Measurement of rotating beam vibration using optical (dic) techniques. Procedia Eng. **199**, 477–482 (2017)
10. Baqersad, J., Carr, J., Lundstrom, T., Niezrecki, C.: Dynamic characteristics of a wind turbine blade using 3d digital image correlation. Proc. SPIE Int. Soc. Opt. Eng. **8348**, 74 (2012)
11. Liu, Y., Gao, H., Zhuge, J., Zhao, J.: Research of under-sampling technique for digital image correlation in vibration measurement. In: Harvie, J.M., Baqersad, J. (eds.) Shock & Vibration, Aircraft/Aerospace, Energy Harvesting, Acoustics& Optics, vol. 9, pp. 49–58 (2017)
12. Endo, M.T., Montagnoli, A.N., Nicoletti, R.: Measurement of shaft orbits with photographic images and sub-sampling technique. Exp. Mech. **55**, 471–481 (2015)
13. Peeters, B., Van der Auweraer, H., Guillaume, P., Leuridan, J.: The polymax frequency-domain method: a new standard for modal parameter estimation? Shock. Vib. **11**, 395–409 (2004)